Investigation on the control of phosphate leaching by sorption and colloidal transport: Column studies and multi-surface complexation modelling

Ruben Warrinnier[a],[*], Thomas Goossens[a], Fien Amery[b], Thijs Vanden Nest[b], Mieke Verbeeck[a], Erik Smolders[a]

[a] KU Leuven, Department of Earth and Environmental Sciences, Kasteelpark Arenberg 20, B-3001, Leuven, Belgium
[b] Research Institute for Agriculture, Fisheries and Food (ILVO), Crop Husbandry and Environment, Burgemeester Van Gansberghelaan 109, B-9820, Merelbeke, Belgium

ARTICLE INFO

ABSTRACT

Surface complexation modelling (SCM) is a powerful tool to estimate speciation and fate of solutes in soil, provided sufficient model validation. This study aims to describe phosphate (PO_4) leaching with SCM. The leachate phosphorus concentrations ([P]) of 120 unsaturated columns of contrasting agricultural soils were measured and modelled. Leachate [P] ranged 0.7–240 μM. Leachate [P] increased as the ratio of P to iron and aluminium ($\frac{P}{Al+Fe}$) in acid oxalate soil extracts increased and as leachate Fe and Al concentrations ([Al + Fe]) increased. SCM was used to describe PO_4 sorption to ferrihydrite (CD-MUSIC model). This yielded adequate description of leachate [P] ($RMSE_{log10} = 0.39$), but only when reactive PO_4 was described from isotopically exchangeable PO_4, when organic matter was included as the main competing adsorbate and when mobile colloidal ferrihydrite was included. The model reveals that colloidal PO_4 transport enhanced leachate PO_4 concentrations up to a factor 50 at small soil P content and small calcium (Ca^{2+}) concentration in solution, as a large Ca^{2+} concentration enhances colloidal stability. This modelling approach explained that long-term application of organic fertilisers with higher Ca content reduced P leaching, likely due to the effect of Ca^{2+} on colloidal stability. A two-parameter empirical Langmuir model, based on soil Fe and Al oxyhydroxides, fitted data better than any SCM, suggesting that the empirical model might be advocated for application at large scale. This study revealed the power of SCM to better understand colloidal transport of P in soil.

1. Introduction

Phosphate (PO_4) fertiliser application on arable land grew exponentially since the second world war (Cordell et al., 2009). Globally, each year eight million tons phosphorus (P) is lost to water bodies from the total 14 million tons applied to arable land, with eutrophication as a negative consequence hereof (Cordell et al., 2009; Ulén et al., 2007). The PO_4 leaching through the soil profile can be a significant pathway by which P is lost, especially in agricultural lowland regions (Addiscott and Thomas, 2000; Fortune et al., 2005; Schoumans and Groenendijk, 2000; Ulén et al., 2007). There is a high need for models being able to predict PO_4 leaching and assess the efficacy of possible fertiliser application restrictions (Csathó and Radimszky, 2009). However, Hinsinger (2001) concluded that in spite of intensive research, the mobility of inorganic phosphorus in most soils is still rather poorly understood and hardly predictable.

The PO_4 sorption on reactive surfaces, i.e. surfaces of Fe and Al oxyhydroxides, is considered the main process controlling P mobility in agricultural soils (Regelink et al., 2015; Weng et al., 2012, 2011). However, at high pH and high calcium concentrations ([Ca]), Ca-phosphates might precipitate (Weng et al., 2011). Schoumans and Groenendijk (2000) presented a 'Langmuir type' sorption model, based on work of van der Zee and van Riemsdijk (1986), to predict PO_4 leaching from a soil layer, with the acid oxalate extractable iron (Fe_{Ox}), aluminium (Al_{Ox}) and P (P_{Ox}) as input variables. This model was developed and parameterized for non-calcareous sandy soils in the Netherlands. In Flanders (the northern part of Belgium), PO_4 leaching is often thought to be restricted to acid sandy soils in the West Flanders and the Northern Campine region because of their light texture and intense fertiliser application rates (De Bolle et al., 2013). Recently, Vanden Nest et al. (2017) used the P concentration in a 10 mM calcium chloride ($CaCl_2$) soil extract to describe the leachate P concentration from soil columns of sandy loam and loamy soils. Part of the soil samples for these leaching experiments originated from two long-term field trials testing different organic fertiliser types (Vanden Nest et al., 2016). For both trials, P leaching could not be explained based on total

P input only. In contrast, the type of fertiliser affected leaching. In both cases, plots amended with farmyard manure showed elevated P leaching compared to the control and other fertiliser types. Vanden Nest et al. (2016) concluded that this was related to a decrease of the orthophosphate distribution coefficient of the soil as determined in a radiotracer experiment. The underlying cause for this was, however, unclear.

Alternatively to these (semi-)mechanistic and empirical approaches, more sophisticated surface complexation modelling (SCM) can be done and allows to estimate the speciation of P in soil (Hiemstra and van Riemsdijk, 1996). These models were developed and calibrated to model ion sorption in batch systems with pure mineral phases as adsorbents (Antelo et al., 2010; Hiemstra et al., 2013; Rietra et al., 2001; Tiberg et al., 2013; Tiberg and Gustafsson, 2016; Weng et al., 2012, 2008). Recently, efforts are made to use them for predictions in batch systems with natural soil (Cui and Weng, 2013; Hiemstra et al., 2010b; Regelink et al., 2015; Weng et al., 2011). The parameters of surface complexation models, that were calibrated for pure mineral systems, can be combined to predict PO_4 leaching for more complex systems without the use of adjustable parameters.

However, the application of SCM to natural samples is challenging. First, the determination of the reactive PO_4 pool of the soil is necessary as model input and mostly P_{Ox} is used (Cui and Weng, 2013; Gustafsson, 2006, 2001). However, the acid oxalate extraction can dissolve calcium phosphates and can release occluded P from inside the pores of short range ordered Fe and Al oxyhydroxides, resulting in an overestimation of the reactive PO_4 pool. Second, there is a lack of experimental techniques to analyse both the specific surface area of reactive oxide surfaces and the organic matter coating of these surfaces in natural samples (Regelink et al., 2015). This hampers a good description of the competitive interaction between PO_4 and organic matter (OM) anions in binding these surfaces (Regelink et al., 2015; Verbeeck et al., 2017). One way to describe this interaction is by attributing a reference specific surface area to the (oxy)hydroxides in soil and defining OM as a carboxyl anion (RO^-) with a, very large, hypothetical complexation constant (Gustafsson, 2006). The amount of RO^- is then an adjustable parameter of the model. Alternatively, Hiemstra et al. (2010a) developed a modelling method to determine the effective reactive surface area of the oxide fraction (m^2) and the reversible bound phosphate. With this, it was found that oxyhydroxides had nano-sized dimensions (in the range of 1–10 nm) and are embedded in a matrix of organic matter (Hiemstra et al., 2010a, 2010b). To model this, a surface OM species was defined. The amount of this surface OM species, bound on Fe and Al oxyhydroxides, was then fitted for each soil sample (Hiemstra et al., 2013, 2010b; Weng et al., 2011). The relative adsorption of this OM species, i.e. adsorbed OM divided by the sum of adsorbed PO_4 and adsorbed OM (symbol y, $mol\ mol^{-1}$), showed a nonlinear correlation with the organic carbon content of the soils (OC, %): $y = 0.32 log(OC) + 0.27$ ($R^2 = 0.79$) (details in Hiemstra et al., 2010b). Verbeeck et al. (2017) found a similar relationship. The ratio of the fitted OM species (RO^-) to ($Fe_{Ox} + Al_{Ox}$) ($mol\ mol^{-1}$) increased sharply with increasing OC until a plateau is reached: $RO^-/(Fe_{Ox} + Al_{Ox}) = 1.5\ OC/(1 + 4.4\ OC)$ ($R^2 = 0.50$). The nonlinear aspect of these relationships suggests that, after the initial increase of the fraction of organic matter covered surface with OC, a plateau is reached and $RO^-/(Fe_{Ox} + Al_{Ox})$ remains constant (starting from 1% OC) (Verbeeck et al., 2017).

Third, PO_4 can be bound to and transported by mobile Fe and Al oxyhydroxide nanoparticles (1–100 nm) and colloids (1–1000 nm), characterised by a large specific surface area (Regelink et al., 2013; Sharma et al., 2017; Siemens et al., 2004; Vendelboe et al., 2011). Adsorption of OM anions introduces a negative charge on the oxyhydroxide surface, leading to electrostatic and/or steric stabilisation of these colloids. Increasing concentrations of polyvalent ions, such as Ca^{2+}, enhances bridging of these organic-matter-stabilised particles and promotes aggregation, which reduces their mobility (Bollyn et al., 2016; Philippe and Schaumann, 2014). Sjöstedt et al. (2018) found

their geochemical modelling of lead solubility improved when validated to lead concentrations in ultrafiltered (< 10 kDa), instead of 0.45-μm-filtered, soil suspensions. To our knowledge, colloid-mediated PO_4 transport has not yet been incorporated into a SCM framework. This would be a simultaneous description of PO_4 sorption on immobile sorbents in the particulate phase and on mobile colloids in the solution phase.

The objectives of this study are to evaluate the use of SCM to describe phosphate leaching from various soil columns and to better understand the involved mechanisms, including understanding effects of different fertiliser types on P mobility (Vanden Nest et al., 2016). First, data of 962 leachate samples from 120 soil columns were collected and analysed statistically in relation to soil properties. Next, different SCM scenarios, using the state-of-the-art Charge Distribution – Multi Site Competition (CD-MUSIC) model, were tested in their predictive power and compared with (semi-)empirical models.

2. Materials and methods

2.1. Leaching experiments with unsaturated soil columns

The data used are derived from two sets of column experiments: a new set (dataset A, not published before) and a previously published dataset (dataset B; Vanden Nest et al., 2017). Both column experiments were performed identically and the procedure is outlined below.

Dataset A is based on triplicate columns with samples collected from 15 different agricultural soils (n = 45) from Flanders, Belgium. Three soils have a sandy loam texture, seven soils a loamy texture and five a sandy texture. Dataset B originates from leaching experiments with 75 soil columns, filled with 69 different soil samples from 4 different long-term field trials (named Qualiagro, ORG G9/G10, ME10.01 and ME05.01; details in Vanden Nest, 2015). The Qualiagro (1998–2013) and M05.01 (2005–2011) trails were set up to test the agronomic value of different organic fertiliser types and are discussed in previous work (Cambier et al., 2014; Vanden Nest et al., 2016, 2014). In short, eight different fertiliser treatments were compared in the M05.01 trial: mineral fertilisers (MIN), dairy farmyard manure (FYM), dairy cattle slurry (CSL), vegetable, fruit and garden waste compost (VFG), two types of farm compost (CMC1 and CMC2; both contain plant material only, no manure), no fertiliser (NF+) and unfertilized fallow (NF−). The Qualiagro trial consists of five treatments: a compost of green waste and the source-separated organic fraction of municipal waste (BIO), a municipal solid waste compost (MSW), a compost of green waste, wood chips and sewage sludge (GWS), dairy farmyard manure (FYM) and only mineral N fertilisers (CONT).

The common set-up of the leaching experiment is detailed in Vanden Nest (2015). In brief, fresh soil samples, collected from the plough layer (0–30 cm), were mixed and sieved on a 2 cm mesh sieve and stones, earthworms and plant material were removed. Soil columns (diameter 125 mm; height 80 mm) were filled with the equivalent of 1.374 kg dry soil. Artificial rainwater (0.015 mM SO_4^{2-}, 0.04 mM Cl^-, 0.02 mM Ca^{2+}, 0.004 mM K^+, 0.02 mM Na^+, 0.004 mM H^+) was applied at the top of the columns at an average rate of 3.5 mm day^{-1}, while at the bottom, a vacuum pump kept the pressure at 10 kPa below atmospheric pressure (field capacity), yielding unsaturated conditions and water residence times of seven to 47 days, depending on the soil. A Macherey-Nagel GF/D filter (2.7 μm pore diameter) and a glass fibre filter (10–16 μm pore diameter) at the bottom of the columns separated the soil from the applied suction. The leachate was collected and analysed twice a week. The concentration of P was measured in both filtered (< 0.45 μm; $[P]_{0.45}$) and unfiltered leachates ($[P]$) by Inductively Coupled Plasma-Optical Emission Spectroscopy (ICP-OES). For dataset B, iron (Fe) and carbon (C) concentrations were measured in the filtered leachates as well ($[Fe]_{0.45}$ and $[C]_{0.45}$) after sample acidification. The same was done for dataset A with additional measurements of Ca, C, Al and Fe concentrations in unfiltered and filtered, acidified samples (ICP-

OES) ([Ca], [Ca]$_{0.45}$, [C], [C]$_{0.45}$, [Al], [Al]$_{0.45}$, [Fe] and [Fe]$_{0.45}$). The experiments were stopped after about four weeks, which is equivalent to about 1.5–5 eluted pore volumes, depending on the soil sample. All data of the experiments were used, including the so-called first flush upon starting the columns. The total number of leachate samples analysed were 378 (dataset A, 45 columns) and 584 (dataset B, 75 columns).

2.2. Soil analysis

The total organic carbon content (OC, %), the pH of a dried (45 °C) soil sample in 5 mM calcium chloride extract (pH$_{CaCl2}$), Fe$_{Ox}$, Al$_{Ox}$ and P$_{Ox}$ (mmol kg^{-1}) and the P content in a 10 mM CaCl$_2$ extract (P$_{CaCl2}$, mmol kg^{-1}) were determined on all soil samples prior to column operation (details in Table A.1). The orthophosphate distribution coefficient (K$_D$, l kg^{-1}) and the total isotopically exchangeable PO$_4$ pool (E-value, mmol kg^{-1}) were determined in duplicate: 2 g oven-dried (45 °C), sieved (< 2 mm) and crushed soil was added to 19 ml 5 mM CaCl$_2$ solution, the suspension was shaken in the end-over-end shaker for 19 h. Then, 1 ml of a 30 kBq ^{33}PO$_4$ radionuclide solution was added and the samples were remounted on the end-over-end shaker (T = 20 ± 2 °C) for five days. Next, the samples were centrifuged at 2500 RCF for 15 min. In the supernatants, ^{33}PO$_4$ concentrations were measured by liquid scintillation analysis (Perkin Elmer, TriCarb, 2800 TR) and the ^{31}P concentrations by ICP-MS (Inductively Coupled Plasma-Mass Spectroscopy, Agilent 7700x, with use of helium gas in the collision cell to remove interferences). From these data, the K$_D$ and E-value were calculated (1, 2).

$$K_D = \frac{[^{33}P]_{initial} - [^{33}P]_{\text{ five days}}}{[^{33}P]_{\text{five days}}} \frac{L}{S} \tag{1}$$

$$E - value = [^{31}P]\left(K_D + \frac{L}{S}\right) \tag{2}$$

[^{33}P] is the concentration of ^{33}PO$_4$ in solution (Bq/ml), $\frac{L}{S}$ is the liquid/solid ratio of the soil suspension (l kg^{-1}), [^{31}P] is the stable ^{31}P concentration in the supernatants (mM) and K_D is the orthophosphate distribution coefficient (l kg^{-1}).

2.3. Data treatment and correlation analysis

Datasets A and B were pooled and analysed together. Dataset A included Ca and Al measurements and, therefore, the datasets were not identical. All statistical analysis was done with JMP PRO 12 SAS°. To homogenize variation, variables with a skewness coefficient larger than 1 were log$_{10}$ transformed prior to computing correlation matrices, i.e. OC, Al$_{Ox}$, Fe$_{Ox}$, P$_{Ox}$, P$_{CaCl2}$, K$_D$ and the leachate concentrations of all elements. It was visually checked if a lognormal distribution better estimated the observed histograms and confirmed that the skewness of the transformed distribution was inside the [-1; 1] interval.

3. Modelling leachate composition

Based on theory and the correlation analysis, three different approaches were used to describe the leachate P concentrations ([P]). First, a surface complexation model, the CD-MUSIC model (Hiemstra and van Riemsdijk, 1996), was used to evaluate the dominant processes controlling [P] with no calibration to the data, excluding some scenarios as detailed below. Second, sorption of P in soil was described by sorption isotherms that were calibrated with experimental data (termed 'Langmuir-type' models). Finally, an empirical regression model was used to model [P] from P$_{CaCl2}$.

3.1. CD-MUSIC modelling

CD-MUSIC modelling was performed with the Visual Minteq 3.1 geochemical program (Gustafsson, 2016). The CD-MUSIC model was chosen because it is the state-of-the-art model for ion adsorption to oxyhydroxide surfaces and it has been used to account for organic matter-phosphate competition. Following assumptions were made:

3.1.1. Ferrihydrite was chosen as a model species to represent the soil's reactive surface

Ferrihydrite is omnipresent in soils and is more reactive towards PO$_4$ than goethite and hematite because of its high specific surface area and site density (Hiemstra et al., 2010a; Hiemstra and Van Riemsdijk, 2009; Regelink, 2014; Schwertmann and Cornell, 2000; Wang et al., 2013). The sum of Fe$_{Ox}$ and Al$_{Ox}$ (mmol kg^{-1}) was used as a model input for ferrihydrite content in soil. The structural parameters of ferrihydrite are taken from Tiberg et al. (2013) (Table A.3). All surface complexation reactions considered are shown in Table A.3. No distinction was made between Fe and Al oxyhydroxides as there is currently no model available to describe organic matter-phosphate interaction, with a systematic database for sorption reactions, for the latter (Dijkstra et al., 2009; Sjöstedt et al., 2018). Crystalline forms of Fe and Al oxyhydroxides were not considered in the modelling. In agricultural top soils they do not contribute largely to PO$_4$ binding due to their relative low abundance (about 30% of the total Fe content is crystalline (Hiemstra et al., 2010a)) and low specific surface area (typically 10–50 m^2 g^{-1} vs. 650 m^2 g^{-1} for ferrihydrite). In the subsoil and in weathered (tropical) soils, crystalline iron can contribute more (Buekers et al., 2007; Hiemstra et al., 2010a).

3.1.2. Local equilibrium assumption

Water residence times in the columns ranged from 7 to 47 days. This was assumed to be long enough for PO$_4$ desorption from the solid phase to have reached equilibrium.

3.1.3. Composition of the liquid phase

The liquid phase was assumed to consist of the artificial rainwater, except for Ca (see below). Additionally, carbonate was added to the system assuming that pore water was in equilibrium with ten times atmospheric carbon dioxide pressure (White, 2006). Silicic acid was added by assuming that the liquid phase was in equilibrium with a saturated Quartz solution (logK$_s$ = −4). For dataset A, dissolved Ca was fixed at the measured [Ca] and the counter ion was nitrate (NO$_3$$^-$) (having similar complexation constants as Cl$^-$, Table A.3). For dataset B, [Ca] was not measured. Therefore, the average measured [Ca] of dataset A, i.e. 1.102 mM Ca, was assumed for all simulations of dataset B. This simplification has limited effects on predicted [P], i.e. less than a factor two (this is elaborated in section 4.2 and Fig. A.1). The pH was fixed at the measured pH$_{CaCl2}$.

3.1.4. The solid/liquid ratio (S/L) of the unsaturated soil columns is fixed at 4.9 kg l^{-1}

This is an average value. However, model simulations are insensitive to variation in S/L, i.e. there was no relevant change (i.e. less than 1% difference) in the predicted leachate P concentration when S/L was varied from 1.4 to 14 kg l^{-1}.

3.1.5. All leached P is inorganic, either ionic or bound to colloids or particles; organic P species are not present in the leachates

The correlation analysis (see Section 4.1, 5.1 and Fig. 1) supports this assumption. Both Oehl et al. (2004) and Stutter et al. (2015) conclude that P cycling in arable soils is dominated by physicochemical processes with inorganic P.

Six model scenarios (S1 − S6; Table 1) were run, with increasing complexity, to describe 1) the reactive PO$_4$ pool (S1−S2), 2) organic matter-PO$_4$ interactions (S3−S5) and 3) colloid-mediated PO$_4$ transport (S6).

S1 : Oxalate extractable phosphorus (P_{Ox}) is used as model input for total PO_4.

S2 : The isotopically exchangeable PO_4 (E-value) is used as model input for total PO_4.

S3-S5 *organo-mineral associations*: Different approaches to incorporate the sorption of organic matter anions (RO^-) on ferrihydrite are tested. As done in previous work (Gustafsson, 2006; Verbeeck et al., 2017), a surface complexation reaction between a carboxylic group (RO^-) and the ferrihydrite surface was simulated (Table A.3). The $log_{10}K$ value of this reaction was fixed at 25 (Gustafsson, 2006). First (S3), a fixed amount of RO^- was added to all columns, i.e. an average amount of reactive carboxyl groups. This was the only adjustable parameter. In S4, it was hypothesised that the amount of RO^- is correlated with the OC of the soil and one adjustable parameter, i.e. the proportionality factor between RO^- and OC, was used. Finally (S5), RO^- was added as a fixed fraction of ($Fe_{Ox} + Al_{Ox}$), i.e. the total reactive surface. This means that a certain fraction of the soil's reactive surface is assumed to be covered with a coating of organic matter. This fraction of surface coverage is the only adjustable parameter and is equal for all columns.

S6 *Colloidal transport:* This final scenario is as S5 but incorporated colloidal transport to describe [P], i.e. the solution P was the sum of truly dissolved PO_4 and colloidal bound PO_4, without including extra adjustable parameters. If solution [Fe] was oversaturated with respect to ferrihydrite ($log_{10}K_{sp} = 2.69 = log_{10}((Fe^{3+})(H^+)^{-3})$), this concentration was converted to a ferrihydrite concentration in the liquid phase and this was added to the model as an additional reactive surface, with the same structural properties as particulate ferrihydrite in soil. In a second step, to include Al oxyhydroxide colloids in solution, [Al] and [Fe] were summed on a molar basis and both added as precipitated ferrihydrite in the liquid phase. This approach is equivalent to the separate precipitation of Fe as ferrihydrite and Al as an $Al(OH)_3$ ($8.29 = log_{10}((Al^{3+})(H^+)^{-3})$) as in both cases practically all Fe and Al precipitate. For dataset B no [Al] and [Fe] measurements were available. These were estimated from $[Fe]_{0.45}$ using a linear regression that was established for dataset A ($log_{10}([Al]) = 0.82 + 0.76 \, log_{10}([Fe]_{0.45})$, $RMSE_{log} = 0.68 \, log_{10}M$; $log_{10}([Fe]) = 0.28 + 0.97 \, log_{10}([Fe]_{0.45})$, $RMSE_{log} = 0.45 \, log_{10}M$). This estimation did not deteriorate model performance (details not shown). The graphical abstract gives a schematic overview of the modelling approach of scenario 6, which is the most complete, but most complex modelling scenario. In this scenario, P is partitioned between two surfaces: a particulate and a colloidal surface.

3.2. 'Langmuir-type' P leaching models

The 'Langmuir-type' model is based on the surface complexation between PO_4 and the Fe and Al oxyhydroxide ligands (L), present in the soil solid phase (3).

$$PO_{4(aq.)} + L_{(solid)} \leftrightharpoons LPO_{4(solid)} \tag{3}$$

The deduction of the model equation (5) is given in the electronic annex (Section A.1) and summarised below. The concentration of PO_4 in solution ($[PO_4]$ mol l^{-1}) increases nonlinearly with increasing degree of phosphate saturation (DPS, defined as (4)). Here, α is the fraction of Fe_{ox} and Al_{ox} available for PO_4 binding ($-$).

$$DPS = \frac{P_{ox}}{\alpha(Fe_{ox} + Al_{ox})} \tag{4}$$

$$[PO_4] = K^{-1} \frac{DPS}{1 - DPS} \tag{5}$$

This model has two adjustable parameters. α ($-$) and K is the equilibrium constant of the PO_4 sorption reaction (M^{-1}).

Additionally, Langmuir isotherms were fitted for each texture class ('texture specific Langmuir' model). This yields three isotherms and a model with six adjustable parameters. Calibration, i.e. parameter estimation, was performed with MATLAB (Version 9.0–3 march 2016, The MathWorks Inc.). Nonlinear least squares regression to the data (using the Levenberg-Marquardt algorithm) was used to estimate the model parameters (K and α) yielding the lowest sum of squared errors (LSE).

3.3. Model calibration and comparison

Leachate [P] was log_{10} transformed to homogenize the variation and these log_{10} transformed values were used to validate or calibrate the models. The simulations, made in each scenario, were evaluated by plotting predicted $log_{10}[P]$ versus observed $log_{10}[P]$ and using following model validation criteria: the least sum of squared errors (LSE_{log}), the root of the mean squared error ($RMSE_{log}$, 6), the Akaike information criterion (AIC, 7) and the Bayesian information criterion (BIC, 8). The AIC and BIC favour models with less adjustable parameters (p), to prevent overfitting. n is the number of data points.

$$RMSE_{log} = \sqrt{\frac{LSE_{log}}{n}} \tag{6}$$

$$AIC = 2p + n \, ln\left(\frac{LSE_{log}}{n}\right) \tag{7}$$

$$BIC = p \, ln(n) + n \, ln\left(\frac{LSE_{log}}{n}\right) \tag{8}$$

4. Results

4.1. Soil properties and leachate composition

Table A.1 provides the summary statistics of selected soil and leachate properties and Table A.2 the selected soil properties for the soils used in dataset A. Soil OC (%) ranges from 0.9 to 2.2%. The pH_{CaCl2} ranges from 4.2 to 6.5, the degree of phosphate saturation (DPS) from 16 to 69%, P_{CaCl2} from 0.02 to 0.24 mmol kg^{-1}, K_D from 140 to 1555 $l \, kg^{-1}$ and the E-value from 1.3 to 7.4 mmol kg^{-1}. Leachate P concentration ([P]) ranges four orders of magnitude (from 0.7 to 240 μM) out of which 88% exceed 4.5 μM, i.e. the Flemish environmental limit for surface waters. [Fe], [Al] and [Ca] vary as well (0.4–350 μM Fe, 1.1–920 μM Al and 0.1–12 mM Ca).

Upon starting the columns, a transient phase in which [P] changed with time, was generally followed by a phase in which [P] did not change anymore, reached after 0.4 to 1.7 cumulative leached pore volumes. The five distinct panels of Fig. A.2 show respectively [P], $[Fe]_{0.45}$, [Fe + Al], [Ca] and [C] as a function of the cumulative leached water (ml). In general, [P], $[Fe]_{0.45}$ and [Fe + Al] increase during the transient phase, while [Ca] decreases. For some columns, most clearly for column '14' a peak in $[Fe]_{0.45}$ and [Fe + Al] is visible and this peak is associated with a peak in [P].

Fig. 1 shows the results of the correlation analysis for the pooled dataset (A + B). Leachate P concentrations ([P]) most strongly correlate negatively with the orthophosphate distribution coefficient (K_D, $l \, kg^{-1}$; $r = -0.85$) and positively with the degree of phosphate saturation (DPS) of the soil (%; $r = +0.79$). Large [P] is also associated with large $[Fe]_{0.45}$ but this correlation is less strong ($r = +0.46$). For dataset B, [Fe] and [Al] are positively correlated ($r = +0.94$) (Fig. 2). The sum of [Fe] and [Al] ([Fe + Al]) is most strongly, and negatively, correlated with [Ca] ($r = -0.47$), and much less with pH_{CaCl2} ($r = -0.20$). Leachate [P] increases with [Fe + Al] ($r = +0.70$), but only for low P-saturated soils (DPS < 30%). For soils with a higher DPS, the slope of this association
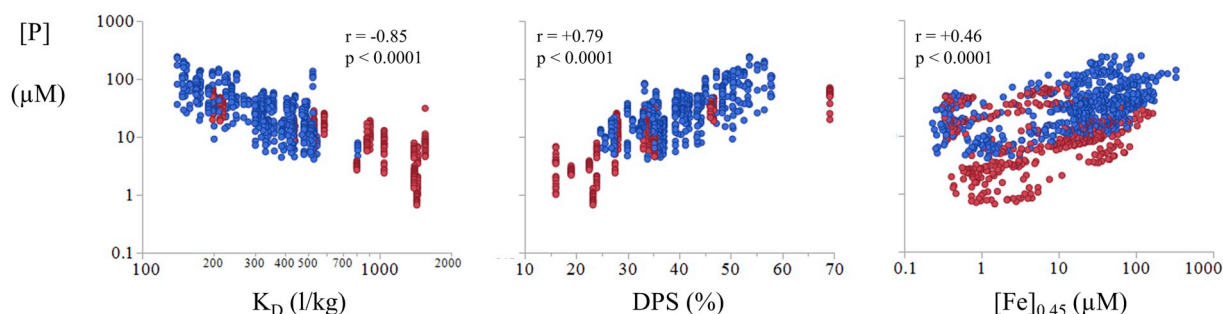
Fig. 1. (colour figure) Correlation analysis of the pooled dataset suggests PO_4 sorption on Fe and Al oxyhydroxides. Starting from left, the first two correlations suggest that PO_4 sorption on poorly crystalline Fe and Al oxyhydroxides controls leachate [P]. The K_D is the orthophosphate solid-liquid distribution coefficient (as measured with $^{33}PO_4$) and represents the affinity of the soil's solid phase to bind PO_4. The degree of phosphate saturation (DPS, %) is calculated as $\frac{P_{ox}}{0.5(Fe_{ox} + Al_{ox})}100\%$. The third correlation, between Fe and P in the leachate, suggests Fe-colloids mediate P leaching. Points in red correspond to dataset A and points in blue to dataset B. Correlation coefficients are given for the pooled dataset (A + B). (For interpretation of the references to colour in this figure legend, the reader is referred to the Web version of this article.)

levels off. The same correlations are present for the concentrations measured in the filtered samples (not shown).

4.2. Surface complexation modelling

Table 1 gives a summary of the modelling results of the different scenarios. The modelled $\log_{10}[P]$ is plotted against the observed values for different model scenarios (Fig. 3). The simplest scenario S1, assuming that P_{Ox} is the reactive PO_4 pool, overestimates [P] by a factor 43, on average. Using the E-value instead (S2), underestimates it by a factor 153, on average. Both S1 and S2 did not incorporate the reactive organic matter (RO^-), which increases leachate [P] due to competition between RO^- and PO_4 for binding on ferrihydrite. Therefore, using P_{Ox} results in even larger overestimations upon including RO^- (data not shown). Therefore, the E-value was used in further scenarios. Incorporating RO^- in various ways improves the description (contrast LSE_{log} S3−S5 with S2 in Table 1). The best fit was obtained in S5, where RO^- was added as a fixed fraction of the total amount of ferrihydrite. Finally, adding colloidal bound P to the model further improves the model performance, with a final root of mean square error ($RMSE_{log}$) of $0.39 \log_{10}(mol\, l^{-1})$ for scenario 6. In a normal distribution, two-third of the points are within one RMSE and 95% are within two times the RMSE. The only adjustable parameter is the fraction of ferrihydrite's surface that is covered by organic matter anions and was optimized to 37% of the singly coordinated surface sites, which corresponds to a molar $RO^-/(Fe_{Ox} + Al_{Ox})$ ratio of 0.22.

To investigate colloid-facilitated PO_4 leaching, the modelled factor-increase in PO_4 leaching due to the presence of colloids was calculated, i.e. this is the predicted total solution $[PO_4]$ with colloids divided by the corresponding predicted concentration without presence of colloids. This ratio was plotted against the concentration of ferrihydrite colloids, entered as model input (Fig. 4). A functional relationship is clear: at large colloid concentrations, leaching of P can be enhanced by colloids by up to a factor 50 compared to the same simulation without colloids. The magnitude of the factor of facilitated transport depends on the PO_4 loading of the colloids. When total observed [P] is low (e.g. 10^{-6} M), colloids largely enhance total P concentrations in the liquid phase; conversely, at large phosphate concentrations (e.g. 10^{-4} M), the relative contribution of colloids to leachate P is smaller, because of PO_4 saturation of the colloids. The solution [Ca] has a strong effect on the presence of colloids and, thus, on the modelled colloidal bound PO_4 (Fig. 5; recall the middle panel of Fig. 2). There is a negative correlation between [Ca] and the colloidal bound PO_4 ($r = -0.54$; $p < 0.0001$). Generally, above 1 mM Ca, colloidal bound PO_4 is below 1 μM.

A univariate sensitivity analysis showed the effect of the different input parameters on predicted [P] by the SCM approach (scenario 6) (Fig. A.1). Predictions were made for the soil column with average properties (red dots) and each input variable was varied across the
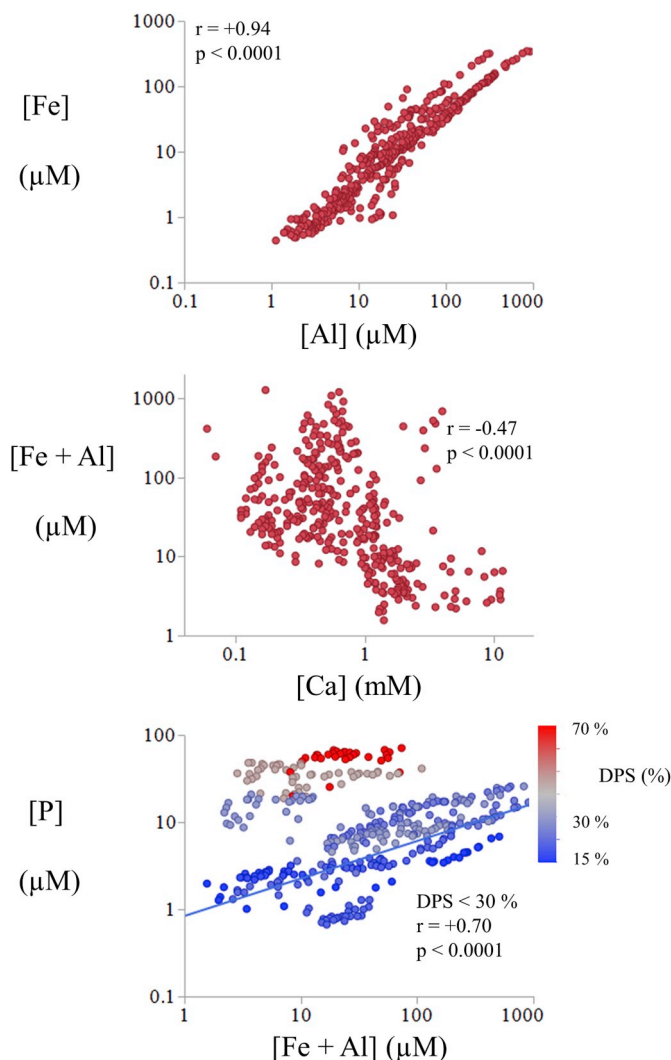

Fig. 2. (colour figure) Correlation analysis of dataset A suggests PO_4 sorption on colloidal Fe and Al oxyhydroxides. The strong correlation between [Fe] and [Al] (top panel) suggests the presence of Fe and Al colloids. Ca^{2+} bridging and flocculation of colloids is suggested by the negative correlation between [Ca] and [Fe + Al] (middle panel). The lower panel shows a strong positive correlation between the [P] and [Fe + Al] for the soils with a degree of P saturation (DPS) below 30%. This suggests colloids mediate P leaching, but only in low P-saturated soils. For soils with DPS > 30%, there is no significant correlation and the slope of the relation levels off. (For interpretation of the references to colour in this figure legend, the reader is referred to the Web version of this article.)

Table 1
Summary of CD-MUSIC modelling scenarios. Scenarios 1 and 2 contain no adjustable parameters, whereas the introduction of organic matter interaction (S3−S6) adds one adjustable parameter in the modelling scenario (indicated by the letter a). Scenario 6, which assumes that organic matter covers a constant fraction of the soil's reactive surface and includes colloid-mediated PO_4 leaching, gives the best description of leachate P concentrations. This is indicated by smallest values for the model validation criteria.

Model scenario				# adj. parameters	n	LSE_{log}	$RMSE_{log}$ $(log_{10}(M))$	AIC	BIC
	Solid phase, particulate Ferrihydrite	reactive PO_4 pool	Organic matter interaction	Colloidal phase, ferrihydrite						
S1	$(Fe_{Ox} + Al_{Ox})$	P_{Ox}	–	–	0	962	1816	1.37	611	611
S2	$(Fe_{Ox} + Al_{Ox})$	E-value	–	–	0	962	4188	2.09	1415	1415
S3	$(Fe_{Ox} + Al_{Ox})$	E-value	a mM RO^-	–	1	962	699	0.85	−305	−300
S4	$(Fe_{Ox} + Al_{Ox})$	E-value	$RO^- = a$ OC (%)	–	1	962	802	0.91	−173	−168
S5	$(Fe_{Ox} + Al_{Ox})$	E-value	$RO^- = a (Fe_{Ox} + Al_{Ox})$	–	1	962	278	0.54	−1193	−1188
S6	**$(Fe_{Ox} + Al_{Ox})$**	**E-value**	**$RO^- = a (Fe_{Ox} + Al_{Ox})$**	**[Fe + Al]**	**1**	**962**	**146**	**0.39**	**−1810**	**−1805**

n: number of leachate samples (observations); # adj parameters: number of adjustable parameters in the models; LSE_{log}, $RMSE_{log}$, AIC and BIC: model validation criteria.

range found in the dataset (Table A.1). Varying the E-value has the largest effect on the predicted [P], which range almost 3 orders of magnitude. The concentrations of particulate and colloidal ferrihydrite ($Fe_{Ox} + Al_{Ox}$ and [Fe + Al] respectively) have the second largest effect. The soil pH has smaller effects, with a maximum of [P] at pH 5.5 (11 μM P) and a minimum at pH 4.2 (8.2 μM). Increasing [Ca], at equal colloid concentrations, decreases [P], but only to a small extent (21 μM P at 0.1 mM Ca and 7.5 μM P at 11.6 mM Ca). Increasing the dissolved Si concentrations has minor effects. The soil moisture content of the soil column (controlled by the soil texture) has negligible effects, i.e. less than 1%, on predicted leachate P concentrations (details not shown).

4.3. (Semi-)empirical approaches for large scale predictions

The results of the calibration of the semi-empirical models are shown in Table A.4. Calibrating the Langmuir-like model for each texture class separately, i.e. the 'texture specific Langmuir' model, resulted in the best fits. The SCM approach describes leachate [P] better than a mere regression between [P] and soil specific P_{CaCl2} data, the latter assumed to represent P present in the soil solution ($RMSE_{log} = 0.39$ versus $RMSE_{log} = 0.46$). However, the general 'Langmuir' model fits the data better than the SCM approach. Table A.5 provides the estimated parameters of the (semi-)empirical models and their 95% confidence intervals. Both α and K differed significantly across the different texture classes. α was highest for the sandy soils (0.38), 0.33 for the loamy soils and lowest for the sandy loam soils (0.30). K was highest for the sandy soils (152 mM^{-1}), intermediate for the sandy loam soils (96 mM^{-1}) and lowest for the loamy soils (68 mM^{-1}).
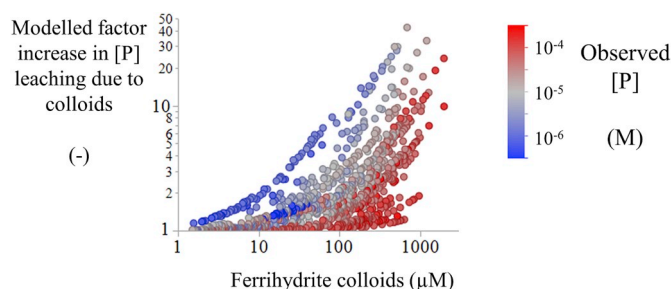
Fig. 4. (colour figure) Colloids facilitate PO_4 leaching. Ferrihydrite colloids, expressed in molar Fe units, enhance leachate [P] up to a factor 50, but mainly for low P-saturated soils (having low total observed [P]). Saturation of the colloids at high total P loads decreases the 'colloidal effect'. (For interpretation of the references to colour in this figure legend, the reader is referred to the Web version of this article.)

4.4. Fertiliser type influences leachate P concentrations

Table A.6 provides the mean soil and leachate properties of the different treatments in the long-term field trials (subset of dataset B). The results of the different fertiliser treatments were discussed by Vanden Nest et al. (2016). In short, soil columns sampled from the green waste, wood chips and sewage sludge (GWS) and the dairy farmyard manure (FYM) treatments from the Qualiagro trial, have larger [P] (p < 0.05) compared to the control (CONT) and other treatments. In the M.05.01 trial, the FYM treatment was associated with large [P] as well. The differences in cumulative P applications per plot in the field did not fully explain the differences in [P] (Fig. A.3). For example, despite the larger P input in the BIO treatment, less P is leached in comparison with FYM. The same holds for M.05.01, where P
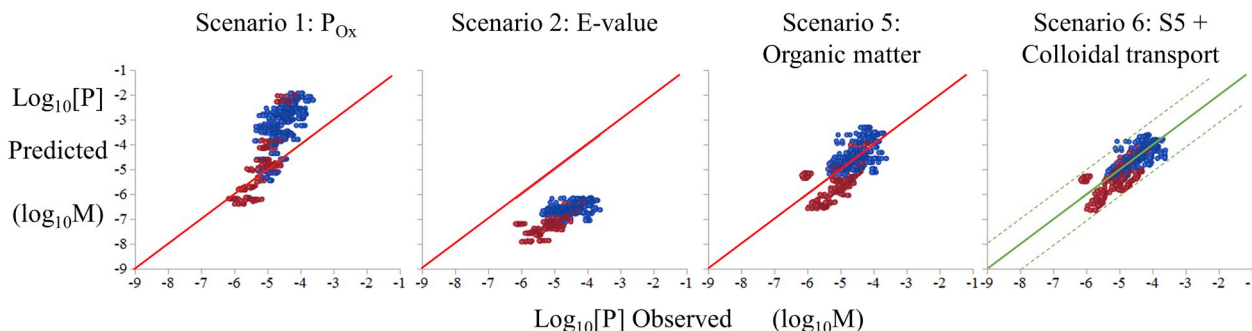
Fig. 3. (colour figure) CD-MUSIC modelling scenarios: predicted versus observed leachate P concentration ([P]). Surface complexation modelling scenario 1 overestimates [P], while scenario 2 results in underestimations. Scenario 5 and scenario 6 both further improve the simulations. See Table 1 for details on the modelling scenarios. Points in red correspond to dataset A and points in blue to dataset B. (For interpretation of the references to colour in this figure legend, the reader is referred to the Web version of this article.)
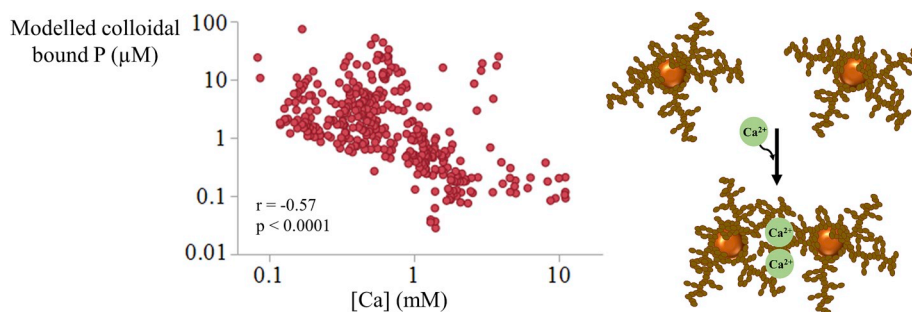
Modelled colloidal bound P (μM)

r = -0.57
p < 0.0001

[Ca] (mM)

Fig. 5. (colour figure) Ca constraints colloidal PO_4 leaching. 'Ca bridging' constraints colloidal PO_4 transport. Above 1 mM Ca, modelled colloidal PO_4 is generally below 1 μM. The modelled colloidal PO_4 is that part of leachate P which is predicted to be bound by colloids. (For interpretation of the references to colour in this figure legend, the reader is referred to the Web version of this article.)

input due to fertilisation does not necessarily involve elevated [P] and only the FYM treatment significantly increased [P] in comparison the zero P input systems. For Qualiagro, all treatments increased the OC content of the soil. The GWS treatment increased Al_{Ox} and P_{Ox}. Interestingly, $[Fe]_{0.45}$, a proxy for colloidal particles, is significantly reduced by the BIO and MSW treatments.

In the M.05.01 trial, similar trends are visible. Organic fertilisation increased OC (%). The most successful SCM scenario S6 can describe leachate P concentration from both trials adequately ($RMSE_{log}$ is 0.21 and 0.20), with successful simulation of the treatment effects. This is shown in Fig. A.3 where the predicted $log_{10}[P]$ represent a subset from the model simulations in scenario 6 of the SCM approach.

5. Discussion

5.1. PO_4 sorption on particulate and colloidal Fe and Al oxyhydroxides controls leachate P concentrations

The correlation analysis suggested two mechanisms are controlling leachate P concentrations, i.e. PO_4 sorption on particulate Fe and Al oxyhydroxides and colloid-mediated PO_4 leaching. These mechanisms were underpinned by the multi-surface complexation modelling (SCM) approach.

First, Fig. 1 suggests that PO_4 sorption on poorly crystalline Fe and Al oxyhydroxides controls leachate [P]. Although already known for acid sandy soils (Del Campillo et al., 1999), SCM now also confirms this for near neutral sandy loam and loamy soils. Second, the large leachate iron concentrations ([Fe]) are most likely indicating mineral colloids, given the strong association with aluminium [Al] (Fig. 2), the very low solubility of iron and aluminium oxyhydroxides (Lofts et al., 2008) and the large exceedance of the solubility products of ferrihydrite and Al(OH)$_3$. However, no direct evidence for colloids is available. This could be addressed in the future via filtration over a smaller pore size. There is an inverse relationship between [Fe + Al], a proxy for colloids, and [Ca] (Fig. 2). Increasing $[Ca^{2+}]$ reduces colloidal stability as Ca^{2+} bridges negatively charged colloidal particles (Bollyn et al., 2016; Philippe and Schaumann, 2014). The statistical association between [Fe + Al] and [P] suggests co-transport, a finding supported by the SCM. Disregarding colloid-mediated PO_4 transport in SCM reduces model performance ($RMSE_{log}$ from 0.38 to 0.54 $log_{10}(M)$). When total leachate [P] is low (blue points in Fig. 4), the contribution of colloid-mediated PO_4 transport to leaching is high. This can be explained because of the nonlinear shape of the sorption isotherm of PO_4 on Fe and Al oxyhydroxide colloids. At low PO_4 saturation, the colloidal fraction of PO_4 in solution is large. Increasing the total PO_4 load saturates the colloids and their affinity for PO_4 drops. This results in a decreased contribution of colloids to PO_4 leaching. This effect is visible in Fig. 4 and in the lower panel of Fig. 2. Colloids enhance PO_4 leaching (Figs. 4 and 5), especially at low [Ca] (below 1 mM) and low [P] (below 10 μM).

To further investigate whether precipitation of Ca-phosphates can be controlling P solubility in the columns, the saturation indices (SI) were calculated (dataset A only) for different calcium-phosphates (CaHPO$_4$, logK = −19.28), tri-calcium-phosphate (Ca$_3$(PO$_4$)$_2$,

logK = −25.5), octa-calcium-phosphate (Ca$_4$H(PO$_4$)$_3$, log K = −47.95) and apatite (Ca$_5$(PO$_4$)$_3$OH, log K = −58.2) (details not shown). All solutions were unsaturated with respect to calcium-phosphate, tricalcium-phosphate and octa-calcium-phosphate. In 16% of the data from dataset A, i.e. four soils, leachate samples were oversaturated with respect to apatite. For these points there was a negative relation between $log_{10}[P]$ and $log_{10}[Ca]$ with a slope of −0.44. If calcium phosphates would control P solubility, stoichiometry dictates a steeper slope (steeper than −1). The Ca^{2+}-bridging, and subsequent flocculation, of organic matter coated colloids is more likely explaining the association between solution P and Ca, as there is a positive relation between $log_{10}[C]$, $log_{10}[Fe + Al]$ and $log_{10}[P]$ for these points (details not shown). Moreover, precipitation of apatite is kinetically inhibited because the more soluble tricalcium-phosphate is needed as a precursor (Regelink et al., 2015). Therefore, we speculate that Ca-phosphates are not controlling P solubility.

5.2. A roadmap for surface complexation modelling (SCM)

5.2.1. The isotopically exchangeable PO_4 pool is a better proxy for the reactive PO_4 pool than oxalate extractable phosphorus

For our dataset, P_{Ox} is about two times larger than the E-value. From both a conceptual and empirical point of view, the E-value is preferred as model PO_4 input, because it represents the pool of PO_4 that is in dynamic interaction with the soil solution and because it is the pool that has the same fate as the freshly added PO_4 which corresponds with the short term PO_4 isotherms on ferrihydrite with which the CD-MUSIC model is calibrated. The P_{Ox} includes occluded P inside the pores of poorly crystalline Fe and Al oxyhydroxides and calcium phosphates (Six et al., 2012). These are not exchangeable within relevant time scales and can, therefore, not contribute to leaching, on the short term. This concept is supported by the SCM, showing that using P_{Ox} results in overestimations of leachate [P] (Fig. 3 and Table 1).

5.2.2. Reactive organic matter in topsoil can be modelled as a function of the total reactive surface

Three different approaches to model organic matter-PO_4 interaction on ferrihydrite were tested. Adding these organic anions (RO$^-$) as a function of OC (%) (S4) did not improve model description compared to a fixed amount of RO$^-$ for every column (S3). Only a small fraction of OC (the reactive humic and fluvic acids) will take part in the sorption reactions. Scenario S5, assuming a constant fraction of RO$^-$-covered-surface, was found to be the best fitting scenario. This confirms previous studies (Hiemstra et al., 2010b; Verbeeck et al., 2017) and points to organo-mineral associations. Because all soils here are collected from the surface layer and have relative large OC content (all above 0.9%), the plateau in the relationship between the fraction of RO$^-$-covered-surface and OC, as found in Verbeeck et al. (2017), is reached. The optimized molar RO$^-$/(Fe + Al)$_{Ox}$ ratio was 0.22; which corresponds to a RO$^-$ loading on the reactive surface of 3.8 μmol m^{-2}. Previous studies reported fitted organic matter ratios ranging from 0.06 to 5.9 μmol m^{-2} in agricultural topsoils, indicating the need for an experimental technique to quantify the organic matter coating on the

soil's reactive surface (Cui and Weng, 2013; Gustafsson, 2006; Hiemstra et al., 2013, 2010b; Regelink et al., 2015; Weng et al., 2011).

5.2.3. Colloid-mediated PO₄ leaching should be incorporated

This leads to the final modelling approach as is depicted in the graphical abstract. Here, [Fe + Al] was used as a proxy for ferrihydrite colloids and is an input parameter for the SCM. However, for this approach, Fe and Al measurements are needed, which are not directly available for large scale predictions in the field.

5.3. Are differences in P leaching among different organic amendments explained?

The SCM might assist the rather complicated interpretation of effects of the type of organic soil amendment on leachate P concentrations in both field trials. Treatment effects were successfully described by SCM (Fig. A.3). In the Qualiagro trial, excessive modelled leachate [P] in the treatment with compost of green waste, wood chips and sewage sludge (GWS) is due to the large E-value, which, in turn, can be explained because of the larger total P input. We recall that this field trial had used 23 years of equal annual carbon input, not equal P input. For the farmyard manure amended soil (FYM), the large E-value is responsible for elevated predicted [P] compared to the unamended control. The high Ca containing fertilisers (BIO and MSW) did not increase leachate [P], despite considerable P input. These applications significantly reduced leachate Fe concentrations ([Fe]$_{0.45}$) in comparison to the control and other treatments. It is hypothesised that this is likely due to Ca^{2+} bridging, as described in section 5.1. The decreased leachate [Fe]$_{0.45}$, compared to [Fe]$_{0.45}$ of the control treatment, reduced predicted [P] by a factor 1.8 for the BIO treatment and by a factor 2 for the MSW treatment. This partly explains why these amendments did not increase leachate [P]. However, the combination of pH, (Al$_{Ox}$ + Fe$_{Ox}$), E-value and colloids concentration determines the model output, i.e. modelled leachate [P]. For example, despite the larger P input in the BIO treatment, less leachate [P] is predicted (and observed) compared to the FYM treatment. This is due to the smaller amount of colloids in BIO versus FYM (explains 30% of the difference) and due to the smaller E-value (explains 40% of the difference). The remaining 30% is explained by larger pH and more Al$_{Ox}$ and Fe$_{Ox}$.

In the M.05.01 trial, the farmyard manure treatment (FYM) showed elevated leachate [P] (Fig. A.3). Model simulations showed the larger E-value of farmyard manure amended soils, as compared with the other treatments, is the responsible SCM input parameter which explains excess predicted [P]. For the other treatments, the E-value, as compared to the control treatment, did not increase enough to increase predicted [P]. The soil chemical reasons for this remain unclear.

5.4. Semi-empirical models are better suited for large scale predictions?

Our surface complexation modelling approach requires many parameters that may hamper its use at large scale in the field. The SCM described leachate P concentration better than the mere P$_{CaCl2}$ data. This is remarkable as P$_{CaCl2}$ mimics P present in soil solution, i.e. the fraction which leaches, but, in hindsight, is explained by the variable colloidal P contribution to leaching in the columns, a factor absent in the 10 mM CaCl$_2$ extract. This highlights the good performance of the SCM approach. However, the 'Langmuir-type' model, only based on an acid oxalate extraction, outperforms SCM (Table A.4). Indeed, SCM requires 7 input parameters and consists of many fixed model parameters (e.g. specific surface area of ferrihydrite, the equilibrium reaction constants, the site densities and the layer capacitances). Measurement error on each of these variables likely obscures modelled leachate [P] and introduces considerable error on these. The simplicity of the 'Langmuir-type' model might be its greatest benefit. The underlying concepts were already presented by Schoumans and Groenendijk in 2000. Moreover, for practical purposes SCM is not feasible, as [Fe]

and [Al] in the leachate are necessary input variables and likely exhibit seasonal variability related to actual ionic strength or Ca^{2+} concentrations, requiring leachate samples. Calibration further improves when a Langmuir isotherm is fitted for every texture class separately, indicating that physical factors, such as porosity and water flow, might influence leachate [P].

5.5. Environmental significance and implications for management

The validity of this study and the developed models should be investigated at field scale. A weakness might be the shortcoming of using columns as a model for P leaching in the field. The columns in this study used disturbed soil samples, not intact (undisturbed) soil horizons, and therefore disregard processes such as preferential flow (Jarvis, 2007), stagnant water and associated redox reactions affecting P mobility (Gu et al., 2017), and bioturbation (Rubæk et al., 2013). Probably more important are the large number of pore volumes used in the columns, that decreased pore water [Ca] and thereby enhanced colloidal movement. However, the results from this study can guide management in limiting P leaching and avoiding eutrophication. To limit colloid-mediated PO₄ leaching, pore water Ca^{2+} concentrations should be above 1 mM. If this is not the case, applying Ca as a soil amendment to constrain colloidal mobility can be considered.

6. Conclusions

Taken together, the surface complexation modelling (SCM) can explain the leached P concentrations from unsaturated soil columns with contrasting properties. The leachate P concentration is controlled by PO₄ sorption on poorly crystalline Fe and Al oxyhydroxides. Colloids mediate PO₄ leaching, especially when solution Ca drops below about 1 mM. Ca-rich fertilisers reduce the amount of mobile colloids and, therefore, reduce PO₄ leaching. For predictions at a larger scale, the parameter poor Langmuir model based on Fe and Al oxyhydroxides in soil is the preferred model for P leaching.

Declarations of interest

None.

Appendix A. Supplementary data

Supplementary data to this article can be found online at https://doi.org/10.1016/j.apgeochem.2018.12.012.

References

Addiscott, T.M., Thomas, D., 2000. Tillage, mineralization and leaching: phosphate. Soil Tillage Res. 53, 255–273. https://doi.org/10.1016/S0167-1987(99)00110-5.
Antelo, J., Fiol, S., Pérez, C., Mariño, S., Arce, F., Gondar, D., López, R., 2010. Analysis of phosphate adsorption onto ferrihydrite using the CD-MUSIC model. J. Colloid Interface Sci. 347, 112–119. https://doi.org/10.1016/j.jcis.2010.03.020.
Bollyn, J., Nijsen, M., Baken, S., Joye, I., Waegeneers, N., Cornelis, G., Smolders, E., 2016. Polyphosphates and Fulvates Enhance Environmental Stability of PO 4 -Bearing Colloidal Iron Oxyhydroxides. J. Agric. Food Chem. 64, 8465–8473. https://doi.org/10.1021/acs.jafc.6b02425.
Buekers, J., Van Laer, L., Amery, F., Van Buggenhout, S., Maes, A., Smolders, E., 2007. Role of soil constituents in fixation of soluble Zn, Cu, Ni and Cd added to soils. Eur. J. Soil Sci. 58, 1514–1524. https://doi.org/10.1111/j.1365-2389.2007.00958.x.
Cambier, P., Pot, V., Mercier, V., Michaud, A., Benoit, P., Revallier, A., Houot, S., 2014. Impact of long-term organic residue recycling in agriculture on soil solution

composition and trace metal leaching in soils. Sci. Total Environ. 499, 560–573. https://doi.org/10.1016/j.scitotenv.2014.06.105.

Cordell, D., Drangert, J.-O., White, S., 2009. The story of phosphorus: Global food security and food for thought. Global Environ. Change 19, 292–305. https://doi.org/10.1016/j.gloenvcha.2008.10.009.

Csathó, P., Radimszky, L., 2009. Two Worlds within EU27: Sharp Contrasts in Organic and Mineral Nitrogen–Phosphorus Use, Nitrogen–Phosphorus Balances, and Soil Phosphorus Status: Widening and Deepening Gap between Western and Central Europe. Commun. Soil Sci. Plant Anal. 40, 999–1019. https://doi.org/10.1080/00103620802693151.

Cui, Y., Weng, L., 2013. Arsenate and Phosphate Adsorption in Relation to Oxides Composition in Soils: LCD modeling. Environ. Sci. Technol. 47, 7269–7276. https://doi.org/10.1021/es400526q.

De Bolle, S., De Neve, S., Hofman, G., 2013. Rapid redistribution of P to deeper soil layers in P saturated acid sandy soils. Soil Use Manag. 29, 76–82. https://doi.org/10.1111/j.1475-2743.2012.00426.x.

Del Campillo, M.C., Van Der Zee, S.E.A.T.M., Torrent, J., 1999. Modelling long-term phosphorus leaching and changes in phosphorus fertility in excessively fertilized acid sandy soils. Eur. J. Soil Sci. 50, 391–399. https://doi.org/10.1046/j.1365-2389.1999.00244.x.

Dijkstra, J.J., Meeussen, J.C.L., Comans, R.N.J., 2009. Evaluation of a Generic Multisurface Sorption Model for Inorganic Soil Contaminants. Environ. Sci. Technol. 43, 6196–6201. https://doi.org/10.1021/es900555g.

Fortune, S., Lu, J., Addiscott, T.M., Brookes, P.C., 2005. Assessment of phosphorus leaching losses from arable land. Plant Soil 269, 99–108. https://doi.org/10.1007/s11104-004-1659-4.

Gu, S., Gruau, G., Dupas, R., Rumpel, C., Crème, A., Fovet, O., Gascuel-Odoux, C., Jeanneau, L., Humbert, G., Petitjean, P., 2017. Release of dissolved phosphorus from riparian wetlands: Evidence for complex interactions among hydroclimate variability, topography and soil properties. Sci. Total Environ. 598, 421–431. https://doi.org/10.1016/j.scitotenv.2017.04.028.

Gustafsson, J.P., 2016. Visual MINTEQ 3.1.

Gustafsson, J.P., 2006. Arsenate adsorption to soils: Modelling the competition from humic substances. Geoderma 136, 320–330. https://doi.org/10.1016/j.geoderma.2006.03.046.

Gustafsson, J.P., 2001. Modelling competitive anion adsorption on oxide minerals and an allophane-containing soil. Eur. J. Soil Sci. 52, 639–653. https://doi.org/10.1046/j.1365-2389.2001.00414.x.

Hiemstra, T., Antelo, J., Rahnemaie, R., Riemsdijk, W.H. van, 2010a. Nanoparticles in natural systems I: The effective reactive surface area of the natural oxide fraction in field samples. Geochem. Cosmochim. Acta 74, 41–58. https://doi.org/10.1016/j.gca.2009.10.018.

Hiemstra, T., Antelo, J., van Rotterdam, A.M.D., Debby, van Riemsdijk, W.H., 2010b. Nanoparticles in natural systems II: The natural oxide fraction at interaction with natural organic matter and phosphate. Geochem. Cosmochim. Acta 74, 59–69. https://doi.org/10.1016/j.gca.2009.10.019.

Hiemstra, T., Mia, S., Duhaut, P.-B., Molleman, B., 2013. Natural and Pyrogenic Humic Acids at Goethite and Natural Oxide Surfaces Interacting with Phosphate. Environ. Sci. Technol. 47, 9182–9189. https://doi.org/10.1021/es400997n.

Hiemstra, T., van Riemsdijk, W.H., 1996. A Surface Structural Approach to Ion Adsorption: The Charge Distribution (CD) model. J. Colloid Interface Sci. 179, 488–508. https://doi.org/10.1006/jcis.1996.0242.

Hiemstra, T., Van Riemsdijk, W.H., 2009. A surface structural model for ferrihydrite I: Sites related to primary charge, molar mass, and mass density. Geochem. Cosmochim. Acta 73, 4423–4436. https://doi.org/10.1016/j.gca.2009.04.032.

Hinsinger, P., 2001. Bioavailability of soil inorganic P in the rhizosphere as afffected by root-induced chemical changes: a review. Plant Soil 237, 173–195. https://doi.org/10.1023/A:1013351617532.

Jarvis, N.J., 2007. A review of non-equilibrium water flow and solute transport in soil macropores: principles, controlling factors and consequences for water quality. Eur. J. Soil Sci. 58, 523–546. https://doi.org/10.1111/j.1365-2389.2007.00915.x.

Lofts, S., Tipping, E., Hamilton-Taylor, J., 2008. The chemical speciation of Fe(III) in freshwaters. Aquat. Geochem. 14, 337–358. https://doi.org/10.1007/s10498-008-9040-5.

Oehl, F., Frossard, E., Fliessbach, A., Dubois, D., Oberson, A., 2004. Basal organic phosphorus mineralization in soils under different farming systems. Soil Biol. Biochem. 36, 667–675. https://doi.org/10.1016/j.soilbio.2003.12.010.

Philippe, A., Schaumann, G.E., 2014. Interactions of Dissolved Organic Matter with Natural and Engineered Inorganic Colloids: A review. Environ. Sci. Technol. 48, 8946–8962. https://doi.org/10.1021/es502342r.

Regelink, I., 2014. Natural Nanoparticles in Soils and their role in organic-mineral interactions and colloid-facilitated transport. Wageningen University.

Regelink, I.C., Koopmans, G.F., van der Salm, C., Weng, L., van Riemsdijk, W.H., 2013. Characterization of Colloidal Phosphorus Species in Drainage Waters from a Clay Soil Using Asymmetric Flow Field-Flow Fractionation. J. Environ. Qual. 42, 464. https://doi.org/10.2134/jeq2012.0322.

Regelink, I.C., Weng, L., Lair, G.J., Comans, R.N.J., 2015. Adsorption of phosphate and

organic matter on metal (hydr)oxides in arable and forest soil: a mechanistic modelling study. Eur. J. Soil Sci. 66, 867–875. https://doi.org/10.1111/ejss.12285.

Rietra, R.P.J.J., Hiemstra, T., van Riemsdijk, W.H., 2001. Interaction between Calcium and Phosphate Adsorption on Goethite. Environ. Sci. Technol. 35, 3369–3374. https://doi.org/10.1021/es000210b.

Rubæk, G.H., Kristensen, K., Olesen, S.E., Østergaard, H.S., Heckrath, G., 2013. Phosphorus accumulation and spatial distribution in agricultural soils in Denmark. Geoderma 209–210, 241–250. https://doi.org/10.1016/j.geoderma.2013.06.022.

Schoumans, O.F., Groenendijk, 2000. Modeling soil phosphorus levels and phosphorus leaching from agricultural land in the Netherlands. J. Environ. Qual. 29, 111–116.

Schwertmann, U., Cornell, R.M., 2000. Iron oxides in the laboratory preparation and characterisation, second. WILEY-VCH, Weinheim.

Sharma, R., Bella, R.W., Wong, M.T.F., 2017. Dissolved reactive phosphorus played a limited role in phosphorus transport via runoff, through flow and leaching on contrasting cropping soils from southwest Australia. Sci. Total Environ. 577, 33–44. https://doi.org/10.1016/j.scitotenv.2016.09.182.

Siemens, J., Ilg, K., Lang, F., Kaupenjohann, M., 2004. Adsorption controls mobilization of colloids and leaching of dissolved phosphorus. Eur. J. Soil Sci. 55, 253–263. https://doi.org/10.1046/j.1365-2389.2004.00596.x.

Six, L., Pypers, P., Degryse, F., Smolders, E., Merckx, R., 2012. The performance of DGT versus conventional soil phosphorus tests in tropical soils - An isotope dilution study. Plant Soil 359, 267–279. https://doi.org/10.1007/s11104-012-1192-9.

Sjöstedt, C., Löv, Å., Olivecrona, Z., Boye, K., Kleja, D.B., 2018. Improved geochemical modeling of lead solubility in contaminated soils by considering colloidal fractions and solid phase EXAFS speciation. Appl. Geochem. 92, 110–120. https://doi.org/10.1016/J.APGEOCHEM.2018.01.014.

Stutter, M.I., Shand, C.A., George, T.S., Blackwell, M.S.A., Dixon, L., Bol, R., MacKay, R.L., Richardson, A.E., Condron, L.M., Haygarth, P.M., 2015. Land use and soil factors affecting accumulation of phosphorus species in temperate soils. Geoderma 257–258, 29–39. https://doi.org/10.1016/j.geoderma.2015.03.020.

Tiberg, C., Gustafsson, J.P., 2016. Phosphate effects on cadmium(II) sorption to ferrihydrite. J. Colloid Interface Sci. 471, 103–111. https://doi.org/10.1016/j.jcis.2016.03.016.

Tiberg, C., Sjöstedt, C., Persson, I., Gustafsson, J.P., 2013. Phosphate effects on copper(II) and lead(II) sorption to ferrihydrite. Geochem. Cosmochim. Acta 120, 140–157. https://doi.org/10.1016/j.gca.2013.06.012.

Ulén, B., Bechmann, M., Fölster, J., Jarvie, H.P., Tunney, H., 2007. Agriculture as a phosphorus source for eutrophication in the north-west European countries, Norway, Sweden, United Kingdom and Ireland: a review. Soil Use Manag. 23, 5–15. https://doi.org/10.1111/j.1475-2743.2007.00115.x.

van der Zee, S.E.A.T.M., van Riemsdijk, W.H., 1986. Sorption kinetics and transport of phosphate in sandy soil. Geoderma 38, 293–309.

Vanden Nest, T., 2015. Long term use of different organic fertilizer types and impact on phosphorus leaching. KU Leuven.

Vanden Nest, T., Ruysschaert, G., Vandecasteele, B., Houot, S., Baken, S., Smolders, E., Cougnon, M., Reheul, D., Merckx, R., 2016. The long term use of farmyard manure and compost: Effects on P availability, orthophosphate sorption strength and P leaching. Agric. Ecosyst. Environ. 216, 23–33. https://doi.org/10.1016/j.agee.2015.09.009.

Vanden Nest, T., Vandecasteele, B., Ruysschaert, G., Cougnon, M., Merckx, R., Reheul, D., 2014. Effect of organic and mineral fertilizers on soil P and C levels, crop yield and P leaching in a long term trial on a silt loam soil. Agric. Ecosyst. Environ. 197, 309–317. https://doi.org/10.1016/j.agee.2014.07.019.

Vanden Nest, T., Vandecasteele, B., Ruysschaert, G., Merckx, R., 2017. Prediction of P concentrations in soil leachates: Results from 6 long term field trials on soils with a high P load. Agric. Ecosyst. Environ. 237, 55–65. https://doi.org/10.1016/j.agee.2016.12.015.

Vendelboe, A.L., Moldrup, P., Heckrath, G., Jin, Y., De Jonge, L.W., 2011. Colloid and phosphorus leaching from undisturbed soil cores sampled along a natural clay gradient. Soil Sci. 176, 399–406. https://doi.org/10.1097/SS.0b013e31822391bc.

Verbeeck, M., Hiemstra, T., Thiry, Y., Smolders, E., 2017. Soil organic matter reduces the sorption of arsenate and phosphate: a soil profile study and geochemical modelling. Eur. J. Soil Sci. 68, 678–688. https://doi.org/10.1111/ejss.12447.

Wang, X., Liu, F., Tan, W., Li, W., Feng, X., Sparks, D.L., 2013. Characteristics of phosphate adsorption-desorption onto ferrihydrite: comparison with well-crystalline Fe (hydr)oxides. Soil Sci. 178, 1–11. https://doi.org/10.1097/SS.0b013e31828683f8.

Weng, L., Van Riemsdijk, W.H., Hiemstra, T., 2012. Factors Controlling Phosphate Interaction with iron oxides. J. Environ. Qual. 41, 628–635. https://doi.org/10.2134/jeq2011.0250.

Weng, L., Van Riemsdijk, W.H., Hiemstra, T., 2008. Humic Nanoparticles at the Oxide−Water Interface: Interactions with Phosphate Ion Adsorption. Environ. Sci. Technol. 42, 8747–8752. https://doi.org/10.1021/es801631d.

Weng, L., Vega, F.A., Van Riemsdijk, W.H., 2011. Competitive and synergistic effects in pH dependent phosphate adsorption in soils: LCD modeling. Environ. Sci. Technol. 45, 8420–8428. https://doi.org/10.1021/es201844d.

White, R.E., 2006. Principles and practice of soil science, fourth ed. Blackwell Publishing.